

M. Leuchner *, A. Menzel and H. Werner

Fachgebiet für Ökoklimatologie, Technische Universität München, Freising, Germany

1. INTRODUCTION

The quantity and quality of solar radiation play a vital role for growth and competition within forest ecosystems. Radiation directly affects the increase of biomass by its intensity within the spectral band of photosynthesis. Moreover, it regulates growth by means of absorption in the blue and red fraction of the solar spectrum by pigments of phytoelements (Smith, 1994). Morphogenetic processes, architecture and space sequestration in the canopy due to intra- and inter-specific competition are controlled by the state of the phytochrome photoequilibrium that can be derived from the red / far red - ratio (R/FR; photon fluence rate between 655 and 665 nm divided by photon fluence rate between 725 and 735 nm) as well as by other photoreceptors with absorption maxima in the UV-A and blue region (Ammer, 2003; Smith, 2000). Thus, the spectral band ranging from 350 nm to 800 nm is referred to as morphogenetically active radiation (MAR) (Combes et al., 2000; Varlet-Grancher et al., 1993) which triggers or inhibits processes such as seed germination, stem growth, leaf expansion and orientation, flowering, and dormancy (Grant, 1997; Endler, 1993). Thus, R/FR can be used as a measure of light quality due to its strong correlation to the state of phytochrome photoequilibrium. The MAR also plays an important role in terms of the natural and artificial regeneration at the stand ground by triggering morphogenetic processes.

The radiation field within the canopy and at the ground level of a forest stand is spatially and temporarily highly variable. This heterogeneity refers to light quantity as well as light quality. It is caused by wavelength-selective reflection, transmission, and absorption of the photons, depending on stand structure, species composition and density, phenological growth stage, and the radiation field above the canopy (De Castro, 2000; Baldocchi et al., 1984). For a realistic characterization of spatially highly variable growth dynamics and competition in mixed stands, detailed parametrization of radiation, especially of crucial spectral bands, is required.

The necessary assessment of light quantity and quality with high spatial, temporal, and spectral resolution requires a large number of fairly small-sized detectors measuring both intensity and spectral composition of incoming solar radiation. For three-dimensional objects, such as plants and phytoelements, radiation is appropriately quantified as photon fluence rate (PFR), i.e. photons intercepted by a sphere of unit cross section per unit time (Björn and Vogelmann, 1996; Björn, 1995; Smith, 1982; Smith and Morgan, 1981). In order to measure photons omnidirectional, planar sensors are of limited value. By contrast, detectors with spherical characteristics are needed (Björn and Vogelmann, 1996; Björn, 1995; Smith, 1994; Hartmann, 1978; Byrne, 1966). Progress in optical and electronic micro-technique has paved the way for the development of a multichannel system for measuring the radiation field within a stand with high resolution in respect to wavelength, space and time (Leuchner et al., 2005).

This abstract describes the development, calibration, experimental setup, and some results of a system, applying a quasi-monolithic miniature spectrometer as the central module and 126 (and later 130) spherical radiation sensors deployed in a mixed stand of a mature Norway spruce (*Picea abies* [L.] Karst) and European beech (*Fagus sylvatica* L.) forest in Southern Germany.

2. METHODS

A novel multi-sensor monitoring system based on fiber optic technology and a diode array spectrometer was developed for measuring the radiation field within a 30 m tall mature mixed Norway spruce (*Picea abies* [L.] Karst) - European beech (*Fagus sylvatica* L.) forest stand in Southern Germany. At six levels and a total of 130 positions within an area of 25 m x 25 m the respective amount of radiation within the photosynthetically and photomorphogenetically relevant waveband from 360 nm to 1020 nm was determined by spatially-integrating spherical sensors near-simultaneously with a high spectral resolution of 0.8 nm. The measurements were performed over more than one year continuously.

2.1 Spherical detectors for spectral analysis

The applied sensors are based on multi-modal step-index fiber optic cables (FOC) with 0.6 mm core diameter of quartz glass, 0.06 mm silicone cladding

* Corresponding author address: Michael Leuchner, Ökoklimatologie, Technische Universität München, Am Hochanger 13, 85354 Freising, Germany, e-mail: leuchner@met.forst.tu-muenchen.de

and 0.1 mm nylon coating (Type Optran PWF 600 N, CeramOptec GmbH, Germany). The sensor head consists of abraded, cavity-free solid spheres of 10 mm diameter of white Polyoxymethylene (POM) with a central hole, into which the end of the respective FOC is bonded. The depth of this hole determines the directional characteristics of the sensor. A depth of 4.6 mm was empirically found to be optimal. Silica fiber has excellent optical characteristics and low attenuation values within the desired spectral waveband between 360 nm and 1020 nm. The wavelength-selective detection limit of 40 m silica FOC has been determined to be less than 0.2 W/m^2 (Reitmayer et al., 2002). All FOC endings need to be polished with a high degree of accuracy to minimize reflection losses at the incidence of radiation. A special device was constructed for face grinding of each FOC ending in eight steps. The polish grinding was accomplished by moving the FOC ending to a grinding disk with attached Al_2O_3 -films of eight different grain sizes from $30 \mu\text{m}$ to $0.05 \mu\text{m}$ by means of a micrometer screw.

2.2 Experimental setup

The sensor heads are capable of receiving the PFR from the entire solid angle ($4\pi \text{ sr}$) less the FOC interface. The FOCs lead the photons to a high precision multiplexer matrix. A quasi-monolithic miniature multichannel spectrometer (Zeiss MCS module UV-VIS-NIR) with a diode array of 1024 diodes is installed on top of two high precision stages with electrodynamical linear drives (PMT160-100-EDLM01, Fa. Feinmess Dresden GmbH, Germany). An entire spectrum (190 – 1023 nm with 0.8 nm spectral resolution), of which the waveband 360 – 1020 nm is calibrated and used, can thus be recorded within fractions of a second. The two precision stages are set up perpendicularly to operate as an X-Y-scanner in conjunction with the spectrometer. The positioning accuracy of the X-Y-stages is $< 2 \mu\text{m}$. Each of the 130 positions of the FOCs is sequentially encountered within a total measuring cycle of approx. 2 minutes. The incoming radiation is measured by means of a special linking fiber adapter attached to the MCS module. The gap between the linking adapter and the FOC ending is 0.1 mm. Fig. 1 illustrates schematically the core of the system including the spectrometer, the two precision cross stages, the matrix plate, and the coupled FOCs.

Within the stand the sensors are arranged in a quasi-regular grid consisting of 25 vertical ropes at which the sensors are attached within six vertical levels at 3, 14, 17, 20, 23 and 26 m height (level 1, ground level; levels 2 - 5, canopy levels; level 6, above canopy level).

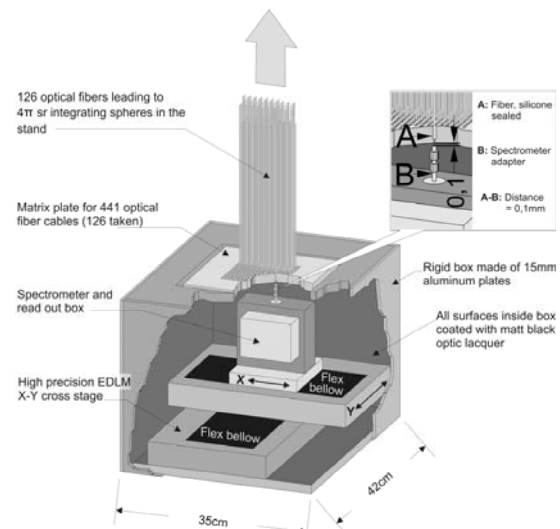


Fig. 1. Schematic of the spectrometer housing with integrated channel multiplexer.

2.3 Calibration and directional characteristics

For acquisition of the actual PFRs in the field, wavelength specific calibration coefficients and the directional characteristics at different angles of incidence need to be determined for the respective sensor. Thus a highly precise calibration procedure based on the description of Bernhard (1993) has been established. Each sensor was calibrated at 30 positions with different angles of incidence and three repetitions with a spectral resolution of 0.8 nm, within the waveband of 360 – 1020 nm. The resulting directional characteristics of the respective sensor can be expressed by a mean coefficient of variation of 2.0% within the whole waveband with a minimum in the red and far red (650 – 750 nm). The reproducibility of the calibration was determined to be 1.7% for the band of biologically active radiation (400 – 800 nm).

A more detailed description of the calibration procedure can be found at Leuchner et al. (2005).

3. RESULTS AND DISCUSSION

The obtained results of which some are shown in the following chapters, demonstrate the capability of the described system in providing highly resolved information about the radiation field within a mature mixed stand with respect to wavelength, space and time. For a more detailed description of the results, in particular of the relationship between light quality and light availability, see Leuchner et al. (2007).

3.1 Comparison between the spherical and flat plate detectors

Due to the spherical shape of the sensor heads with this system, PFR is measured rather than photon flux density (PFD) that is obtained by flat-plate cosine-

corrected sensors. Fig. 2 shows the signal ratio of the spherical detectors compared to standard flat-plate detectors (LI-190SZ Quantum Sensor, LI-COR Inc., USA) above the crown and at the forest floor at clear sky (CS) and overcast sky (OVC) conditions in the course of a day. Spherical sensors within and below the crown receive on average about twice the number of photons than flat-plate detectors independent of meteorological conditions (only OVC conditions plotted). Above the crown at CS conditions the ratio can increase almost up to 6 at lower solar altitude. Comparative measurements of PFR and PFD were also carried out by Björn and Vogelmann (1996) for the photosynthetically active waveband and agree well with our own data. The ratios mainly depend on sky conditions, solar altitude, and aerosol content, thus revealing the importance of the type of measurement performed. In ecological studies, the measurement of PFR is more appropriate (Smith and Morgan, 1981; Hartmann, 1978), i.e. the application of directionally independent sensors such as spherical sensors is rather necessary (Björn and Vogelmann, 1996; Björn, 1995; Smith, 1982; Kubín, 1971; Byrne, 1966).

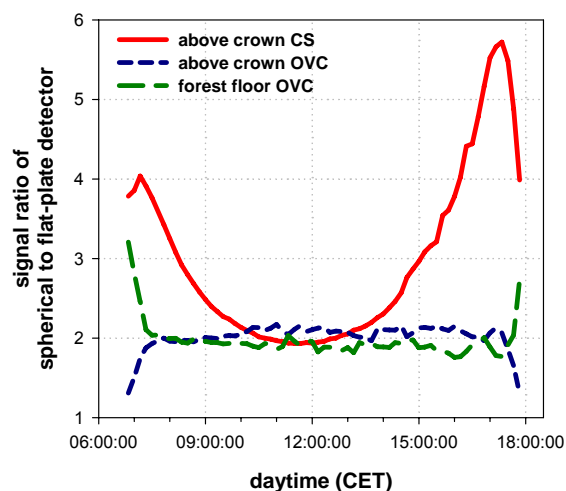


Fig. 2. Signal ratio of the spherical sensors compared to standard flat-plate detectors (LI-COR LI-190SZ Quantum Sensor) in the course of a day under different meteorological conditions (clear sky, CS; overcast sky, OVC) above the crown and at the forest floor.

3.2 Frequency distributions of light availability

The relevance of sunflecks and different shading levels for growth and regeneration of stands due to its strong temporary enhancement of PFR has been emphasized by many studies (Ammer, 2003; Smith, 2000; Grant, 1997). The described system allows an investigation of sunflecks and penumbral stages in terms of frequency distributions of different wavebands of the relative PFR. In Fig. 3 the photosynthetically active (PAR: 400 - 700 nm) and the

far red - near infrared ranges (NIR: 700 - 1000 nm) from below the canopy are examined during full foliage of beech, with a distinction of cases regarding sky conditions and species. Besides the frequency distribution of PFR_{rel} in classes of 0.01, additional information about arithmetic mean, median, 10% and 90% percentile is indicated.

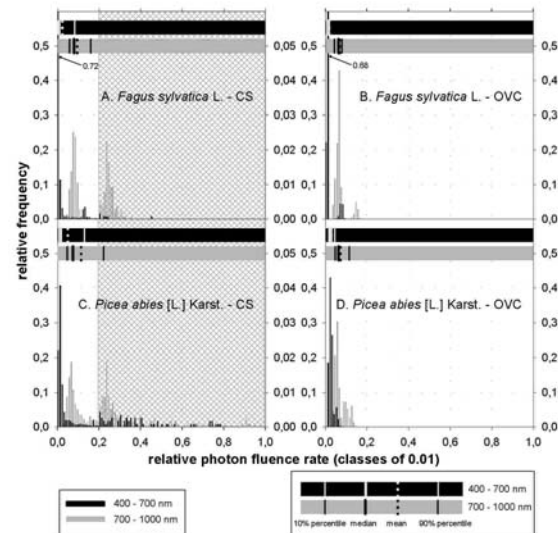


Fig. 3. Frequency distribution of the relative photon fluence rate (PFR_{rel}) (classes of 0.01) within two wavebands (PAR: 400-700 nm; NIR: 700-1000 nm) below the canopy. Hatched area: relative frequency * 10.

Due to the selective absorption of foliage the waveband beyond 700 nm exceeds the photosynthetically active band in all cases. The CS conditions indicate a bimodal distribution of NIR, with a main peak at low PFRs and a secondary maximum between 20% and 30% of PFR. The subordinate peak signifies sunflecks. Due to low solar elevation and the dense stand, with an average projected LAI of 6.2 $m^2 m^{-2}$ and only small gaps (Reiter, 2004) the full amount of downward directed radiation cannot penetrate the stand to the ground. Thus sunflecks should rather be referred to as penumbra or penumbral sunflecks.

3.3 The relationship between light quality and light availability

Within a tree stand, various studies found evidence of a relationship between light quality and light availability (Capers and Chazdon, 2004; Muraoka et al., 2001; Olesen, 1992; Lee, 1987) which is represented in our study by the R/FR and the relative photosynthetic PFR ($PPFR_{rel}$), respectively. Capers and Chazdon (2004) proposed a method of assessing understory light availability rapidly by measuring the light quality in a wet tropical forest. The obtained relationship between percent diffuse transmittance and the R/FR was logarithmic with a high coefficient of determination ($R^2 = 0.97$). Further proof for a

quantitative relationship between the R/FR and the logarithm of the percentage of full sunlight photosynthetic photon flux density (PPFD) was presented by Lee (1989, 1987) for two neotropical rainforests and a tropical moist deciduous forest with R^2 -values above 0.95 for all cases. Muraoka et al. (2001) found a similar, however not quantified relationship for different types of vegetation canopies (Riparian deciduous, coniferous, evergreen, and cool-temperate deciduous forests). No quantitative relationships have been published for mixed forests in temperate climates and the distinction between different conditions at different phenological stages so far.

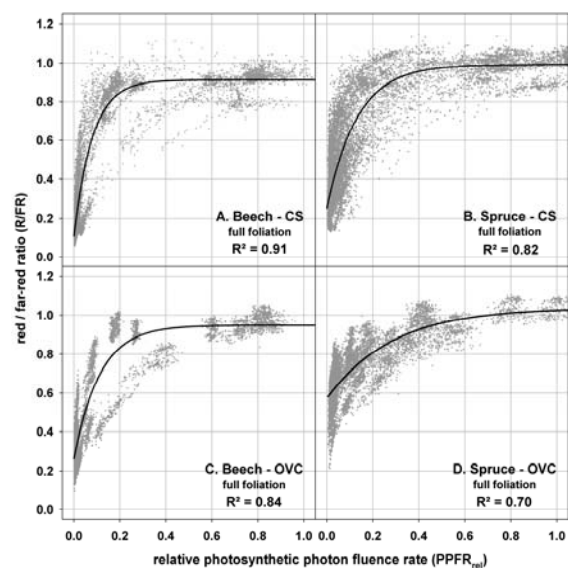


Fig. 4. $PPFR_{rel}$ against R/FR within a Norway spruce - European beech crown at different sky conditions (CS: A, B; OVC: C, D). Investigated period: July 07 - 15 at full foliage.

Fig. 4 shows the relationship of light availability to light quality for a period of full foliage of beech. To minimize the influence of solar altitude on the achieved relationships, only measured values between 09:00 h and 15:00 h CET were considered. In total, all measurements in all sensor heights were assigned. The relationship is following a rectangular hyperbola that was found to give the best-fit regression equation to the distribution for all investigated cases. The basic function with an exponential rise to a R/FR saturation value with increasing $PPFR_{rel}$ has the following shape:

$$\zeta = a + b(1 - e^{-c\Phi}),$$

with ζ = red / far-red ratio and Φ = relative photosynthetic photon fluence rate.

The shape of the function varies with species, sky condition, and state of foliage. The coefficients of determination are higher for the beech functions than for the spruce canopy during foliage while the relationship is opposite as the deciduous trees lose their leaves (not shown). CS conditions are related to

higher coefficients of determination than OVC conditions, independent of the investigated tree species and time period. Beech shows a clear annual variation in the magnitude of correlation. Maximum values of the coefficient of determination ($R^2 = 0.91$ at CS, $R^2 = 0.84$ at OVC) can be found in Fig. 4 at full foliage. The annual minimum ($R^2 = 0.75$ at CS, $R^2 = 0.54$ at OVC) lies at leafless conditions. The highest R^2 of all cases ($R^2 = 0.91$) can be detected at CS conditions and full foliage within the beech canopy.

The results offer a method to derive and assess important parameters for the light climate of temperate forests whose acquisition usually would require much experimental effort with regard to different sky conditions at different phenological stages separated by species. A detailed description of the relationship during different phenological stages can be found at Leuchner et al. (2007).

3.4 Characterization of phenological processes by radiation properties

One objective is the characterization of different phenological stages by investigating properties and changes of the radiation field. During leaf fall and leaf unfolding, daily mean values (due to the increased influence of low solar altitude in the early morning and late afternoon this period was limited to 09:00 - 15:00 h CET) of $PPFR_{rel}$ and R/FR were compared to senescence and shoot rating data (Löw and Weigt, 2005) In particular R/FR shows good correlation for all heights within the canopy (Fig. 5) and thus can be used as an indicator of the phenological stage of those processes.

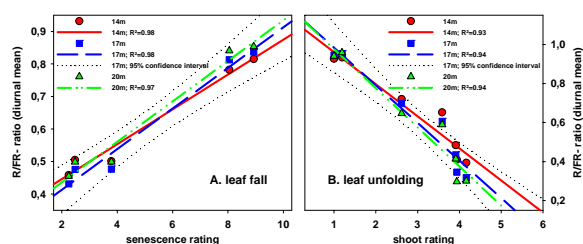


Fig. 5. Comparison of diurnal means of R/FR and according senescence / shoot rating data from leaf fall and leaf unfolding.

3.5 Spectral modeling of the radiative transfer within the mixed forest stand

In addition to the highly resolved spectral measurements, the radiation field in the stand can also be modeled, using an adapted radiative transfer model described by Knyazikhin et al. (1997). The adaption was performed for the implementation of a spectral resolution and the addition of the output of the R/FR. Fig. 6 is an example of the model output for a cross-section just below the canopy of the

investigated stand. For the whole stand 60 cross-sections in 0.5 m resolution are determined for both PPFR and R/FR.

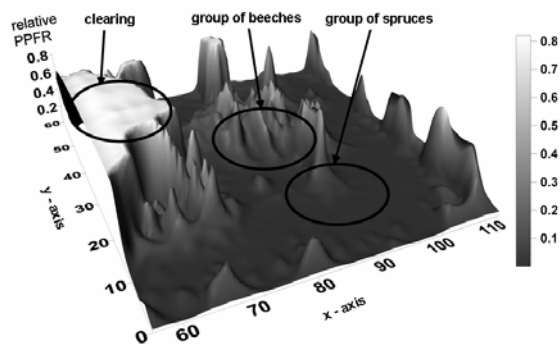


Fig. 6. Model output for the $PPFR_{rel}$ for a profile below the canopy (12 m below tree tops) during full foliage of beech.

Acknowledgements. We gratefully acknowledge the financial support granted by the Sonderforschungsbereich 607 (SFB607) funded by Deutsche Forschungsgemeinschaft (DFG) and the Bayerisches Staatsministerium für Landwirtschaft und Forsten.

4. REFERENCES

- Ammer, C., 2003. Growth and biomass partitioning of *Fagus sylvatica* L. and *Quercus robur* L. seedlings in response to shading and small changes in the R/FR-ratio of radiation. *Ann. For. Sci.* 60, 163-171.
- Baldocchi, D.D., Matt, D.R., Hutchinson, B.A., McMillen, R.T., 1984. Solar radiation within an oak-hickory forest: an evaluation of the extinction coefficients for several radiation components during fully-leaved and leafless periods. *Agric. For. Meteorol.* 32, 307-322.
- Bernhard, G., 1993. Einfluß von Diffusor-Eigenschaften auf die Bestimmung von Bestrahlungsstärken im UV-Bereich: Versuchsaufbau, Messung und Korrekturverfahren. IFU Schriftenreihe Band 22-93, Garmisch-Partenkirchen.
- Björn, L.O., 1995. Estimation of fluence rate from irradiance measurements with a cosine-corrected sensor. *J. Photochem. Photobiol. B: Biol.* 29, 179-183.
- Björn, L.O., Vogelmann, T.C., 1996. Quantifying Light and Ultraviolet Radiation in Plant Biology. *Photochem. Photobiol.* 64, 403-406.
- Byrne, G. F., 1966. A simple way of improving the angular response of solid-state photodetectors. *Agric. Meteorol.* 3, 367-368.
- Capers, R.S., Chazdon, R.L., 2004. Rapid assessment of understory light availability in a wet tropical forest. *Agric. For. Meteorol.* 123, 177-185.
- Combes, D., Sinoquet, H., Varlet-Grancher, C., 2000. Preliminary measurement and simulation of the spatial distribution of the Morphogenetically Active Radiation (MAR) within an isolated tree canopy. *Ann. For. Sci.* 57, 497-511.
- De Castro, F., 2000. Light spectral composition in a tropical forest: measurements and model. *Tree Physiol.* 20, 49-56.
- Endler, J.A., 1993. The color of light and its implications. *Ecol. Monogr.* 63, 1-27.
- Grant, R.H., 1997. Partitioning of biologically active radiation in plant canopies. *Int. J. Biometeorol.* 40, 26-40.
- Hartmann, K.M., 1978. Aktionspektrometrie. In: Hoppe, W., Lohmann, W., Markl, H., Ziegler, H. (Eds.), *Biophysik - Ein Lehrbuch*: Springer, Berlin, Heidelberg, New York, pp. 197-222.
- Knyazikhin, Y., Mießen, G., Panforyov, O., Gravenhorst, G., 1997. Small-scale study of three-dimensional distribution of photosynthetically active radiation in a forest. *Agric. For. Meteorol.* 88, 215-239.
- Kubín, Š., 1971. Measurement of Radiant Energy. In: Šesták, Z., Čatský, J., Jarvis, P.G. (Eds.), *Plant Photosynthetic Production - Manual of Methods*. Dr. W. Junk N.V. Publishers, The Hague, pp. 702-765.
- Lee, D.W., 1989. Canopy dynamics and light climates in a tropical moist deciduous forest in India. *J. Trop. Ecol.* 5, 65-79.
- Lee, D.W., 1987. The spectral distribution of radiation in two neotropical rainforests. *Biotropica* 19, 161-166.
- Leuchner, M., Menzel, A., Werner, H., 2007. Quantifying the relationship between light quality and light availability at different phenological stages within a mature mixed forest. *Agric. For. Meteorol.* 142, 35-44.
- Leuchner, M., Fabian, P., Werner, H., 2005. Spectral multichannel monitoring of radiation within a mature mixed forest. *Plant Biol.* 7, 619-627.
- Löw, M., Weigt, R., 2005. pers. communication.
- Muraoka, H., Hirota, H., Matsumoto, J., Nishimura, S., Tang, Y., Koizumi, H., Washitani, I., 2001. On the convertibility of different microsite light availability indices, relative illuminance and relative photon flux density. *Funct. Ecol.* 15, 798-803.
- Olesen, T., 1992. Daylight spectra (400-740 nm) beneath sunny, blue skies in Tasmania, and the effect of a forest canopy. *Austral. J. Ecol.* 17, 451-461.
- Reiter, I.M. (2004): Space-related resource investments and gains of adult beech (*Fagus sylvatica*) and spruce (*Picea abies*) as a quantification of aboveground competitiveness. Dissertation. Freising.

- Reitmayer, H., Werner, H., Fabian, P., 2002. A novel system for spectral analysis of solar radiation within a mixed beech-spruce stand. *Plant Biol.* 4, 228-233.
- Smith, H., 2000. Phytochromes and light signal perception by plants - an emerging synthesis. *Nature* 407, 585-591.
- Smith, H., 1994. Sensing the light environment: the functions of the phytochrome family. In: Kendrick, R.E., Kronenberg, G.H.M. (Eds.), *Photomorphogenesis in plants - 2nd edition*. Kluwer Academic Publishers, Dordrecht, Boston, London, pp. 377-416.
- Smith, H., 1982. Light quality, photoperception, and plant strategy. *Ann. Rev. Plant Physiol.* 33, 481-518.
- Smith, H., Morgan, D.C., 1981. The spectral characteristics of the visible radiation incident upon the surface of the earth. In: Smith, H. (Ed.), *Plants and the daylight spectrum*. Academic Press, London, New York, Toronto, Sydney, San Francisco, pp. 3-20.
- Varlet-Grancher, C., Moulia, B., Sinoquet, H., Russel, G., 1993. Spectral modification of light within plant canopies. In: Varlet-Grancher, C., Bonhomme, R., Sinoquet, H. (Eds.), *Crop structure and light microclimate: characterization and application*. INRA, Versailles, pp. 427-452.